Title: Ubiquitin-dependent modification of skeletal muscle by the parasitic nematode, *Trichinella spiralis*.

Short Title: Secretion of a Ub E2 enzyme by a parasitic worm

Authors:

White RR[1], Ponsford AH[2], Weekes MP[3,4], Rodrigues R[4], Ascher DB[5,6], Mol M[7], Selkirk ME[1], Gygi SP[4], Sanderson CM[2], Artavanis-Tsakonas K[7*]

Affiliations:

[1] Department of Life Sciences, Imperial College London, UK

[2] Department of Cellular and Molecular Physiology, Institute of Translational Medicine, University of Liverpool

[3]Cambridge Institute for Medical Research, University of Cambridge, UK

[4] Department of Cell Biology, Harvard Medical School, Boston

[5] Department of Biochemistry, University of Cambridge, UK

[6] Department of Biochemistry, University of Melbourne, Australia

[7] Department of Pathology, University of Cambridge, UK

Contact Information:

*ka447@cam.ac.uk

Abstract:

Trichinella spiralis is a muscle-specific parasitic worm that is uniquely intracellular. *T. spiralis* reprograms terminally differentiated skeletal muscle cells causing them to de-differentiate and re-enter the cell cycle, a process that cannot occur naturally in mammalian skeletal muscle cells, but one that holds great therapeutic potential.

Although the host ubiquitin pathway is a common target for viruses and bacteria during infection, its role in parasite pathogenesis has been largely overlooked. Here we demonstrate that the secreted proteins of *T. spiralis* contain E2 Ub-conjugating and E3 Ub-ligase activity. The E2 activity is attributed to *Ts*UBE2L3, a novel and conserved *T. spiralis* enzyme located in the secretory organ of the parasite during the muscle stages of infection. *Ts*UBE2L3 cannot function with any *T.spiralis* secreted E3, but specifically binds to a panel of human RING E3 ligases, including the RBR E3 ARIH2 with which it interacts with a higher affinity than the mammalian ortholog UbcH7/UBE2L3. Expression of *Ts*UBE2L3 in skeletal muscle cells causes a global downregulation in protein ubiquitination, most predominantly affecting motor, sarcomeric and extracellular matrix proteins, thus mediating their stabilization with regards to proteasomal degradation. This effect is not observed in the presence of the mammalian ortholog, suggesting functional divergence in the evolution of the parasite protein. These findings demonstrate the first example of host-parasite interactions via a parasite-derived Ub conjugating enzyme; an E2 that demonstrates a novel muscle protein stabilization function.

Author Summary

Parasitic worms often establish long-lasting infections in their hosts; tightly regulating their surroundings to strike a delicate balance between host cell modulation and protection that will ensure their replication. This is accomplished via the active secretion of parasite glycolipids and glycoproteins into the host. *Trichinella spiralis*, a parasitic nematode that infects skeletal muscle of mammals, birds and reptiles, is the only parasitic worm with a true intracellular stage. *T. spiralis* invade terminally differentiated myotubes, reprogramming them to de-differentiate and re-enter the cell cycle, a process that cannot occur naturally in mammalian skeletal muscle cells, but one that holds great therapeutic potential. We have identified and characterized a novel *T. spiralis* secreted

53 protein that, despite a high level of sequence identity, appears to have evolved a
54 different function to its host ortholog. This protein is an active Ub conjugating enzyme
55 that binds to a panel of human E3 Ub ligases with higher affinity than the host ortholog.
56 Furthermore, when expressed in skeletal muscle cells in culture, its presence uniquely
57 leads to the stabilization of muscle-specific proteins via the downregulation of their
58 ubiquitination.
59
60 **Introduction**
61 The ubiquitin (Ub) pathway is essential for post-translational protein regulation in
62 eukaryotic cells, controlling many important cellular processes such as transcription, cell
63 cycle, differentiation and apoptosis ([1,2]. Ub is a 76 amino acid protein that, in a highly
64 regulated fashion, is covalently conjugated to substrate proteins via an E1 activating, E2
65 conjugating and E3 ligating enzyme cascade[3]. Ubiquitination regulates the fate and
66 function of the substrate, to maintain a healthy homeostasis within the cell. The
67 particular outcome is determined by a combination of possible variables, for example the
68 specific lysine residue attachment site on the protein, the length and type of Ub chain,
69 and the number of total Ub moieties on a single protein[4,5]. Since the specific E2:E3
70 enzyme pair denotes substrate and moiety specificity, ubiquitination is highly regulated
71 by the abundance, localization and activity of these Ub-specific enzymes.
72
73 Considering the important role of the Ub pathway in maintaining the healthy homeostasis
74 of a cell, and therefore the healthy physiology of an organism, it is not surprising that its
75 disruption is directly implicated in infection and disease. Prokaryotes do not have an
76 endogenous Ub pathway, however certain viral and bacterial pathogens encode Ub-
77 specific enzymes that target host Ub machinery for enhanced virulence and immune
78 evasion[6–9]. Although much attention has been aimed at understanding the role of the

Ub pathway in infection by pathogenic viruses and bacteria, very little is known about how parasites may interfere with host ubiquitination. Parasites are eukaryotic and therefore already express endogenous Ub machinery. To date, there are only two reports of the direct targeting of the host Ub pathway during parasitic infection. The first involves indirect communication with the host Ub system by the *Toxoplasma* dense granule protein GRA16. GRA16 is exported into the host cell nucleus and binds the host Ub hydrolase HAUSP, modulating the cell cycle via HAUSP-dependent p53 regulation[10,11]. The second involves direct communication with the host Ub pathway by a *Trypanosoma cruzi* active RING domain secretory protein SPRING. Hashimoto *et al* showed that *in vitro*, SPRING is able to catalyze Ub conjugation with human UbcH5 and 13.

Trichinella spiralis is a promiscuous parasitic nematode that infects skeletal muscle cells of mammals, birds and reptiles. The parasite is propagated by the consumption of infected tissue and undergoes the same life cycle stages irrespective of the host. The longest life cycle stage is intracellular, giving the parasite direct access to host intracellular machinery. The severity of the associated disease, trichinellosis, depends on the infection load and the presentation varies in severity correspondingly from asymptomatic to fatal. During the chronic intracellular phase of infection, *T. spiralis* invade terminally differentiated (TD) myotubes, releasing a mixture of secreted products (SP) including glycoproteins and glycolipids into the cytoplasm and nucleus of the host cell. The host cell undergoes a dramatic program of de-differentiation and cell cycle re-entry followed by cell cycle arrest, initiated and characterized by a change in transcriptional profile, a downregulation of host muscle specific proteins such as myogenin and myosin heavy chain and the loss of identity and function as a myotube[12,13]. This coincides with a change in morphology, as the cell is transformed

from a long, linear fiber into a fat, oval-shaped structure termed a nurse cell ([14–16]. The parasite resides inside the nurse cell until a chance transmission occurs. It is thought that this process of nurse cell development is induced by the *T. spiralis* SP via direct communication with host cell proteins and genetic material.

In this study we used muscle-stage *T. spiralis* as a model to investigate whether eukaryotic parasites have evolved strategies to target the Ub pathway during infection. Not only does *T. spiralis* SP contain both E2 Ub conjugating and E3 Ub ligase activity, we were able to attribute the E2 activity to the secretion of *Ts*UBE2L3, an enzyme that is located in the secretory organ of *T. spiralis* during infection. We show that *Ts*UBE2L3 interacts with the host E3 ARIH2 with higher binding affinity than the endogenous mammalian ortholog. Furthermore, *Ts*UBE2L3 causes a significant downregulation in the levels of ubiquitination of motor, sarcomeric and extracellular matrix proteins. These findings demonstrate the first example of host-parasite interaction via a parasite-derived Ub conjugating enzyme that can stabilize skeletal muscle-specific proteins by inhibiting their ubiquitination.

Results

Intracellular-stage *T. spiralis* secreted products (SP) demonstrate Ub conjugation and ligation activities

An *in vitro* Ub conjugation assay was carried out to determine if the secreted products (SP) of *T. spiralis* muscle larvae contain E1, E2 or E3 enzymatic activity. All reactions were separated by SDS-PAGE and analyzed by streptavidin blot (Figure 1A). As a

positive control, a reaction containing human recombinant E1 (*Hs*UBE1A), human recombinant E2 (*Hs*UBE2L3), and human recombinant E3 (parkin) was analyzed. In the presence of *Hs*UBE2L3, parkin (51 kDa) was able to auto-ubiquitinate, visible as a streptavidin-reactive smear (Figure 1A). When *Hs*UBE2L3 was removed from the reaction no signal was observed (b), confirming the requirement of the E2 for parkin auto-ubiquitination. *T. spiralis* SP were then substituted into the reaction for either the E2, E3 or E1. A reaction containing *T. spiralis* SP plus *Hs*UBE1A only was also analyzed, as well as a reaction containing only *T. spiralis* SP and biotin-Ub as a negative control. A streptavidin-reactive smear, representing either parkin-Ub or SP-Ub, was observed when *T. spiralis* SP were substituted in the place of *Hs*UBE2L3. Signal representing SP-Ub was also observed when *T. spiralis* SP were substituted in the place of parkin. No ubiquitination was observed when *T. spiralis* SP were substituted in the place of *Hs*UBE1A, or when the E1 and SP were reacted alone. This suggests that proteins in *T. spiralis* SP have E2 and E3 but not E1 activities. Since these proteins are activated only by the addition of the human E1 plus E2, or the human E1 plus E3, it is unlikely that the *T. spiralis* secreted E2 and E3 can work together without an external enzyme source. It was therefore hypothesized that ubiquitination of substrates by *T. spiralis* muscle larvae SP requires mammalian host E2 or E3 partners.

Proteomic analysis of *T. spiralis* SP identifies a Ub conjugating enzyme, *Ts*UBE2L3

Purified SP were separated by SDS-PAGE and visualised using colloidal-coomassie staining (Figure 1B) prior to manual excision and analysis by LC/MS/MS. Data was then searched against the *T. spiralis* UniProt proteome, its reverse complement, common contaminants of SDS-PAGE and mass spectrometry as well as the rat UniProt proteome. Less than 1% of the protein matches were rat proteins. To validate the data,

157 the experiment was repeated. Peptides from both the first and second experiment were
158 combined and assembled into proteins. The data was cross-referenced with a previous
159 study of the *T. spiralis* secretome by Robinson *et al*. identifying all the same proteins,
160 plus many new ones[17–19]. Proteins previously identified in *T. spiralis* SP using
161 alternative methods were also present amongst the results[20–25]). To avoid
162 contamination with proteins released from dead or dying parasites, uncoiled and floating
163 *T. spiralis* larvae were removed prior to culturing. In addition, to ensure a low level of
164 parasite death, larvae were cultured for 24 h only, before supernatant was collected for
165 SP purification.
166
167 One Ub enzyme match was made to a putative protein: 'ubiquitin-conjugating enzyme
168 E2 L3 (fragment)'. This sequence is annotated as an incomplete open reading frame
169 (ORF) for a UBE2L3 ortholog (UniProt E5S8T6/GI:339240047/ T.sp_00154). UBE2L3,
170 also known as UbcH7, E2-F1, UbcM4, L-UBC and UBCE7, is a UBCc domain Ub
171 conjugating enzyme (Moynihan et al., 1999; Nuber et al., 1996). The annotated fragment
172 ORF for *Ts*UBE2L3 in the database is 145 amino acids in length and lacks a start codon.
173 The UBCc domain of the putative *Ts*UBE2L3 spans the fragment from the first amino
174 acid to the 140th amino acid. Peptides matching *Ts*UBE2L3 were found in the segment
175 of the gel annotated in Figure 1B, corresponding to its predicted size of 17kDa.
176 *Ts*UBE2L3 was predicted to have no signal peptide (signalP, iPSORT), and to be
177 located primarily in the cytoplasm with trace amounts in peroxisomes, nucleus and
178 extracellular space (WolfPSORT scores of 23, 3, 2 and 2, respectively)[26–28]. All
179 protein matches labeled as 'uncharacterized' were further analyzed using BLAST and
180 SMART, and no other Ub enzyme domains were identified.
181
182 **_Ts_UBE2L3 is responsible for the Ub conjugation activity in _T. spiralis_ SP**

The putative *T. spiralis* UBE2L3 sequence contains 62.3% of the same residues as the human UBE2L3. A commercially available antibody raised against a region of the human enzyme with high identity to the *T. spiralis* protein was used to analyze *T. spiralis* SP by immuno-blot for the presence of UBE2L3. Lysate of *T. spiralis* muscle larvae and human HEK 293T cells were also analyzed as positive controls (Figure 2A). In HEK 293T lysate one prominent band was observed, corresponding to the predicted size of the human UBE2L3 isoform 1, which is 17.9 kDa in size[29]. In the lysate of *T. spiralis* muscle larvae, two prominent bands between 15 and 25 kDa were observed. In the *T. spiralis* SP, the most prominent band was observed between 15 and 25 kDa, matching the smaller band in the *T. spiralis* lysate, and the only band in HEK 293T lysate. To test for contaminant proteins released from dead or dying larvae, the samples were reacted with anti-tubulin antibodies. Although present in the *T. spiralis* and human cell lysates, tubulin was not detected in *T. spiralis* SP by immuno-blot or by proteomic analyses of *T. spiralis* SP.

In order to determine the contribution of *Ts*UBE2L3 to the Ub conjugation activity of *T. spiralis* SP, an *in vitro* depletion assay was carried out (Figure 2B). Using resin-bound anti-UBE2L3 antibodies, SP were depleted of *Ts*UBE2L3 using the immuno-precipitation compatible anti-*Hs*UBE2L3 antibodies. As controls, *T. spiralis* SP were depleted using resin-bound BSA and resin-bound anti-tubulin antibodies. Depleted SP samples were then reacted with human parkin in an *in vitro* Ub conjugation assay whereby parkin auto-ubiquitination was analyzed by streptavidin blot. Reduced signal representing Ub conjugation activity was generated by the *Ts*UBE2L3-depleted SP compared to the BSA and anti-tubulin-depleted SP, although signal was not fully depleted due to affinity inefficiency of the antibody. When quantified this amounted to 61% of the total signal from the anti-*Hs*UBE2L3 sample indicating a 3rd of the E2 activity having been depleted

(Figure 2C). Signal was also present in the SP proteins that were eluted from the anti-*Hs*UBE2L3 resin, amounting to the remaining 31% of the total sample signal. Very faint signal was observed in the proteins eluted from the BSA or tubulin resin that (at 11 and 12% of the total, respectively) could indicate background or non-specific binding to the resin. Results show that *Ts*UBE2L3 is responsible for at least a 3rd of the Ub conjugation activity observed in *T. spiralis* SP (Figure 1A).

_Ts_UBE2L3 specifically localizes to the _T. spiralis_ secretory organ during intracellular-stage infection

In order to analyze *Ts*UBE2L3 expression within infected rat skeletal muscle cells (nurse cells) *in situ*, an antibody was developed that could not cross-react with mammalian UBE2L3. Using structural modeling of *Ts*UBE2L3, an N-terminal peptide showing low homology to the corresponding region of the mammalian ortholog (QWRGLLLPDKEPYC) was synthesized and used to raise a *Ts*UBE2L3-specific antibody (Figure 2D). To confirm *T. spiralis*-specific reactivity, and absence of mammalian cross-reactivity, anti-*Ts*UBE2L3 was reacted with *T. spiralis* lysate, *T. spiralis* SP and rat (*rattus norvegicus*-*R.n*) skeletal muscle tissue (SMT) lysate. Signal at the expected size between 15 and 25 kDa was observed in the *T. spiralis* samples, but not in the *R.n*SMT lysate. Histological sections of infected rat skeletal muscle tissue were prepared for immuno-histofluorescence (IHF) analyses using anti-*Ts*UBE2L3 (Figure 2E). Sections were reacted with either anti-*Ts*UBE2L3 or PBS and analyzed by confocal microscopy in order to locate *Ts*UBE2L3 within the nurse cell complex. *Ts*UBE2L3 was clearly and specifically localized to condensed, discrete stacks of secretory cells (stichocytes) inside the secretory organ (stichosome) of each *T. spiralis* larva within nurse cells (Figure 2E and F).

_Ts_UBE2L3 stably expresses in mouse skeletal myotubes and specifically interacts with the mammalian E3 ARIH2

In order to identify potential *Ts*UBE2L3-protein interactions in skeletal muscle cells, transgenic mouse muscle cell (C2C12) lines were generated[30,31]. Since *T. spiralis* infects fully differentiated skeletal muscle cells, it was important to investigate the effects of *Ts*UBE2L3 on myotubes (rather than myoblasts) in culture. The full ORF of *Ts*UBE2L3 was confirmed by RACE-PCR analysis (Figure S1, 2 and 3) and cloned with a hemagglutinin epitope tag into a lentiviral vector, facilitating doxycycline (DOX)-controlled, inducible transgene expression. C2C12 myoblasts were lentivirally transduced with *Ts*UBE2L3-HA, followed by drug selection to create a silent but stable myoblast cell line. In parallel, control transgenic myoblast lines were developed: 1) an empty vector, 2) eGFP-HA, for overexpression of an unrelated protein, and 3) *Mm*UBE2L3-HA, for overexpression of the mouse UBE2L3 ortholog under the same promoter. All cell lines were differentiated into myotubes (Figure 3A) before transgene expression was induced (Figure 3B). *Ts*UBE2L3-HA expression was confirmed by anti-HA immuno-fluorescence (IFA) (Figure 3C) and immuno-blot (IB) after 24 hours (h) of transgene expression (Figure 3D). Reactivity representing *Ts*UBE2L3-HA was observed at the expected size of approximately 17 kDa at 18, 22 and 48 h post-DOX induction, but not before DOX induction (0 h). No reactivity was observed in the empty vector control. IFA analysis also confirmed that in myotubes, *Ts*UBE2L3-HA is cytoplasmic but not nuclear, despite being observed in both the cytoplasm and nucleus of undifferentiated myoblasts (Figure S4). Myotubes expressing *Ts*UBE2L3-HA did not appear morphologically distinct from the empty vector myotubes (Figure S5).

Using anti-HA antibodies, co-immuno-precipitation (IP) from myotubes of all four transgenic cell lines (empty vector, eGFP-HA, *Ts*UBE2L3-HA and *Mm*UBE2L3-HA) was carried out after 24 h of transgene expression. Proteins that co-precipitated with the HA-

tagged bait protein were separated by SDS-PAGE, visualized by silver staining, anti-HA IB (Figure 4A) and analyzed by LC/MS/MS. Data was then searched against the mouse (*Mus musculus*) UniProt proteome, its reverse complement and common contaminants. To validate the data, the experiment was repeated and the two datasets were merged. All proteins co-precipitated from each cell line were cross-referenced. Amongst these, six RING E3 enzymes were identified in the *Ts*UBE2L3 sample, ARIH1, ARIH2, TRIM3, TRIM25, TRIM47 and TRAF7 and one HECT E3, NEDD4 (Figure 4B, Table 1 and Table S1). As validation for successful *Ts*UBE2L3-specific co-IP, expected "reference" proteins were also identified including the bait protein sequence itself (*Ts*UBE2L3), and the mouse UBE1A (Table S1). All E3 proteins that co-precipitated with *Ts*UBE2L3-HA (as well as controls) and all proteins that only co-precipitated with *Ts*UBE2L3-HA (and neither control) can be found in Table S2.

To further investigate the potential for *Ts*UBE2L3 to interact with human E3-RING proteins, a targeted yeast-2-hybrid (Y2H) interaction screen was performed against a collection of 166 human E3-RING proteins (including one HECT domain ligase E6AP/UBE3A) as previously described (Figure S6 and Table S1)[32,33]. This analysis identified a range of potential *Ts*UBE2L3 interaction partners, observed under low or high stringency conditions (Figure 4B and Table 1). Interactions detected by His3 selection only represent weaker or more transient interactions, while partners detected under combined His3/Ade2 selection represent potentially stronger binary interactions. Notably, a significant proportion of strong, binary interactions were made with members of the non-canonical RING-between-RING (RBR) ligase family (5 out of 13). As the interaction between *Ts*UBE2L3 and the human ARIH2 E3-RBR ligase (also known as ARI1, TRIAD1, Ariadne homologue 2 and All-Trans Retinoic Acid Inducible RING Finger) was detected in both Y2H and co-IP studies, and was the most abundant E3 to co-

precipitate specifically with *Ts*UBE2L3 (Table S2), this high confidence binary complex was therefore selected for further functional characterization.

TsUBE2L3 interacts with RBR ligases with higher affinity than mammalian orthologs

Recombinant 6His-*Hs*ARIH2ΔAri (lacking the auto-inhibitory Ariadne domain) and 6His-*Ts*UBE2L3 (Figure 5A and C) were individually expressed, purified and used for *in vitro* auto-ubiquitination assays. Recombinant 6His-*Ts*UBE2L3 Ub conjugation activity was validated using human parkin (Figure 5B). Interestingly, when reacted at the same concentrations, *Ts*UBE2L3 showed a preference (over human UBE2L3) to catalyze lower forms of parkin-Ub (i.e. mono- and di-Ub) and to lead to more overall Ub conjugation of ARIH2 of which the majority was also observed to be lower form ubiquitination (Figure 5B and D). This ubiquitination pattern coupled with the selective co-precipitation of ARIH2 with *Ts*UBE2L3 led us to speculate that the worm E2 may bind ARIH2 (and possibly other RBR ligases) with a higher affinity than the mammalian ortholog. To test this hypothesis, we generated structural models to investigate the binding affinity of ARIH2 to both TsUBE2L3 and HsUBE2L3.

Modeling the interactions between *Ts*UBE2L3 and *Hs*UBE2L3 with HsARIH2 and Ub revealed differences in residues across the respective interfaces. While *Ts*UBE2L3 shares 67% sequence identity to the human *Hs*UBE2L3, within 5 Å of the >450 Å2 interface with *Hs*ARIH2, all residues except for two are conserved (83% identity) (Figure 5E). However, overall small global changes between the *Ts*UBE2L3 and *Hs*UBE2L3 sequences and structures (r.m.s.d of 0.5 Å) lead to the formation of additional inter-molecular hydrophobic interactions. In addition, Thr2 of *Ts*UBE2L3 is able to make significant interactions with Val144 of *Hs*ARIH2, not made by Ala2 of *Hs*UBE2L3. This is

interesting, as mutation of the corresponding residue in *Hs*ARIH1 (Ile188) has been shown to abolish interaction with UBE2L3[34]. These observations were consistent with predictions by PISA[35] and mCSM-PPI[36] that *Hs*ARIH2 would bind to *Ts*UBE2L3 with higher affinity than *Hs*UBE2L3, with a difference in predicted Gibb's Free Energy of binding of over 1 kCal/mol. By contrast, the larger interface between *Ts*UBE2L3 and *Hs*UBE2L3 with Ub (>900 Å) is less well conserved, with only 58% identity of residues with 5 Å of the interface. Despite this, overall numbers and types of interactions were consistent between the models, with PISA and mCSM-PPI predicting that they would bind Ub with similar binding affinities (difference in predicted Gibb's free energy of binding 0.1 kCal/mol).

Expression of *Ts*UBE2L3 in skeletal muscle cells leads to a downregulation of ubiquitination, markedly of motor, sarcomere and ECM proteins

In order to assess the global effect of *Ts*UBE2L3 on C2C12 myotubes, a ubiquitome analysis was carried out using a post-translational modification (PTM) UbiScan (Ub remnant proteomics) method[37,38]. This method employs the K-ε-GG antibody that binds to the di-Gly motif that remains on a ubiquitinated residue of a trypsin-digested protein (a Ub remnant peptide). This allows enrichment of ubiquitinated peptides from a whole cell lysate for LC/MS/MS analysis. Transgene expression was induced in all four mouse myotube cell lines (empty vector, eGFP, *Ts*UBE2L3 and *Mm*UBE2L3) for 24 h before myotubes were harvested for analysis. Searches were performed against the mouse UniProt proteome and peptide matches were quantified and normalized. To calculate fold change, the abundance and strength of each protein match in a particular sample (eGFP, *Ts*UBE2L3 and *Mm*UBE2L3) was compared to the control sample (empty vector). Results for all three cell lines were filtered to contain only those with a significant fold change of 2.5 or above in response to *Ts*UBE2L3, with a maximum

intensity of 200,000 or above and a maximum % CV of 49.9 or below. Results were categorized based on annotated biological ontology for further analysis (Figure 6A and Table S3). The data was screened for changes in ubiquitination of any of the known mammalian substrates of all strong Y2H E3 partners or E3s that were identified by co-IP (whether known interactors of UBE2L3 or not). None were identified, suggesting an alternate role of TsUBE2L3 to that of its host ortholog.

The ontological group that, overall, displayed the largest specific fold-change in response to *Ts*UBE2L3 expression was composed of proteins known to play a role in motility/contraction, sarcomere structure, extracellular matrix (ECM) and cytoskeleton such as myosin, myomesin, nebulin and troponin. Notably, the majority of proteins that displayed a significant change in ubiquitination in response the *Ts*UBE2L3 expression showed a negative fold-change, i.e. in the *Ts*UBE2L3 column of the heatmap (Figure 6A) fewer ubiquitinated forms of the proteins are observed. This suggests that in the presence of *Ts*UBE2L3, they were either deubiquitinated or not ubiquitinated to begin with (stabilized). We therefore hypothesized that the consequence of this would be observed as a reduction in ubiquitination and a resulting increase in abundance. No significant difference could be observed in the total amount of ubiquitinated protein in *Ts*UBE2L3 cells compared to empty vector myotubes as measured by pull-down of polyubiquitinated proteins using tandem ubiquitin binding motif entity resin (TUBE2, Figure S7A and B). However an increase in the abundance of native myosin II (MYH2) in the *Ts*UBE2L3 myotubes (the protein that showed the largest fold change in ubiquitination specifically in response to *Ts*UBE2L3 expression) was observed by immuno-blot in relation to empty vector cells (Figure 6B and Table S3). This indicates that there is either a reduction in Ub-mediated proteasomal degradation or an increase in expression of particular proteins that remain unaffected in empty vector or

*Mm*UBE2L3 myotubes. Despite an apparent stabilization of proteins important to sarcomere structure, the overall organization of the myotube sarcomere appeared to be disrupted by *Ts*UBE2L3 expression (compared to wild-type, empty vector or *Mm*UBE2L3 myotubes). An IFA assay of the sarcomere Z-disc protein α-actinin, shows a larger proportion of *Ts*UBE2L3 cell structures appearing to be disordered and without characteristic myotube α-actinin-positive stripes. Although quantification is not statistically significant, there appears to be a definite trend of fewer α-actinin-positive stripes in the TsUBE2L3 sample as compared to controls (Figure S7C and D).

Discussion

Various pathogenic viral and bacterial effectors have been identified and characterized as Ub-specific enzymes that successfully manipulate the Ub pathway of the host during infection. Studies in parasites have largely focused on endogenous Ub system components that are important or essential for parasite biology[39–42]). Although these studies demonstrate potential for the identification of novel targets for therapeutic agents, the study of the role of the Ub pathway at the host-parasite interface remains largely uncharted territory. During this study we used *T. spiralis* as an effective model to investigate whether there is a role for the Ub pathway in host-parasite interactions. We identified the first parasite-derived, host-targeted E2 enzyme, *Ts*UBE2L3, setting precedence for the further investigation of the role of parasite Ub conjugation enzymes and the Ub pathway in direct host-parasite interactions. E3 activity was also identified in *T. spiralis* SP, although the identity of the proteins responsible could not be elucidated from conventional LC/MS/MS using the annotated *T. spiralis* proteome. We are currently carrying out further analyses to isolate this activity and identify the protein(s) responsible.

*Ts*UBE2L3 is stored in the secretory organ of *T. spiralis* and is released as an active enzyme by muscle-stage (L1) larvae. In isolated *T. spiralis* SP, the E1, E3 and/or the substrates required for Ub conjugation by *Ts*UBE2L3 are not present, suggesting that this enzyme requires partner components of the Ub conjugation cascade to be provided by an external source. We therefore hypothesized that only when in contact with host partner proteins (i.e. host E3s) does secreted *Ts*UBE2L3 carry out its intended function as an E2 enzyme. As validation of this hypothesis, a number of potential mammalian E3 ligase partners for *Ts*UBE2L3 were identified. The strongest interaction identified was with the RBR ligase ARIH2. Very little is known about the function of RBR ligases such as ARIH2, and to date only one Ub substrate of ARIH2 has been reported in dendritic cells, the NF-κB inhibitor IκBβ[43]. Although human ARIH2 and UBE2L3 are known to interact, ARIH2 was not identified by co-IP as a partner for the mouse UBE2L3 ortholog in skeletal myotubes. When reacted with human parkin *in vitro*, *Ts*UBE2L3 was observed to catalyze more mono-Ub-parkin than the human UBE2L3. When reacted with human ARIH2 *in vitro,* although both E2s showed a preference for lower Ub forms (over poly-Ub forms) of ARIH2-Ub, *Ts*UBE2L3 used at the same concentration was observed to catalyze overall more ubiquitination than *Hs*UBE2L3.

The current accepted mechanism of RBR-mediated Ub conjugation suggests that a Ub-charged E2 binds to the RING1 domain, Ub is then passed on to the RING2 domain, and then onto the substrate. The E2 must then dissociate to allow a new Ub-charged E2 to bind to catalyze any subsequent Ub conjugation that would lead to either Ub chain formation or substrate exchange[44]. Therefore, we postulate that if an E2 binds an RBR more tightly, formation of mono-Ub or lower forms of Ub would be promoted due to the slower dissociation of E2 from E3, i.e. the substrate would be more likely to dissociate/exchange before the E2. Furthermore, the sequestration of the E3 by the E2,

417 could lead to an overall reduction in activity of the E3. It was therefore hypothesized that
418 in our myotube system the parasite *Ts*UBE2L3 has a higher affinity for ARIH2 than the
419 mouse ortholog[45]. The structural modeling results indeed agreed with this hypothesis,
420 showing that the *T. spiralis* E2 makes a more extensive hydrophobic interface with the
421 E3, leading to tighter binding quantified at approximately 1 kCal/mol difference in binding
422 affinities between the human and parasite E2s. It is therefore possible that the parasite
423 UBE2L3 has evolved a higher affinity than the host UBE2L3 in order to outcompete the
424 endogenous enzyme in nurse cells and sequester the host E3 in an inhibitory manner.
425
426 On a cellular level, *Ts*UBE2L3 expression in C2C12 myotubes caused a significant
427 downregulation of ubiquitination of motor, sarcomere and ECM-specific proteins; most
428 notably an effect not observed in response to the expression of the mammalian ortholog.
429 Although this presented as an increase (stabilization) in the abundance of native form of
430 myosin II (MYH2 - the protein with the largest significant fold change in response to
431 *Ts*UBE2L3 expression), the mechanism and physiological effect of this stabilization is
432 yet to be determined. The remodeling of mammalian skeletal muscle tissue is highly
433 regulated by ubiquitination[46–48]. In addition, nurse cell development during *T. spiralis*
434 infection of muscle cells involves dramatic remodeling of the myofibril[49]. Despite
435 previous ultrastructural and biochemical evidence suggesting destruction of myofibrillar
436 proteins in the infected myotube [16,50], the process of nurse cell maintenance is likely
437 very complex. As such, a role for stabilization may be necessary, particularly at later
438 stages of nurse cell development where the L1-stage worm is creating a stable “hideout”
439 within the host cell. Indeed if the regulation of the abundance of the proteins that
440 comprise the sarcomere is essential for proper sarcomere formation, then a significant
441 upregulation in abundance due to a reduction in ubiquitin-mediated turnover may lead to
442 structure disruption as was observed by IFA. Two muscle specific E3 ligases known to

443 be upregulated during muscle remodeling and wasting are Murf1 and atrogin-1. These
444 ubiquitinate structural and motor proteins that are subsequently degraded by the
445 proteasome[51–53]. An interaction between *Ts*UBE2L3 and Murf1 is unlikely given that
446 the mammalian UBE2L3 cannot not interact with Murf1, therefore the loss of myofibrillar
447 proteins seen in previous studies of nurse cells is unlikely to be an effect resulting from
448 *Ts*UBE2L3.
449
450 Since *Ts*UBE2L3 is an E2, it was initially surprising to observe less overall ubiquitination
451 in C2C12 cells expressing the parasite protein. However if the mechanism of interaction
452 of *Ts*UBE2L3 with all host E3 partners is the same as that observed with ARIH2 (namely
453 to bind more tightly than and outcompete the host E2), then inhibitory E3 sequestration
454 may play a role in an overall reduction in ubiquitination of target proteins. It is also
455 possible that *Ts*UBE2L3 acts upstream of a different ubiquitination cascade, perhaps
456 targeting another E2 or E3 as a substrate for degradation that would ordinarily
457 ubiquitinate these proteins. It must be noted that studying the effect of *Ts*UBE2L3 on
458 intact myotubes as opposed to already transformed (*T. spiralis*-infected) cells may not
459 reflect its true biological role during infection or relevant stage during nurse cell
460 formation. The only way to fully assess this would be to generate *Ts*UBE2L3 knock-out
461 parasites, a process that is currently technically impossible until *T. spiralis* is rendered
462 genetically tractable.
463
464 Despite a high level of sequence identity, *Ts*UBE2L3 appears to have evolved a different
465 binding behavior and cellular function to its host ortholog. Functional divergence of
466 orthologous proteins is commonly observed to have evolved between non-pathogenic
467 and pathogenic species of the same lineage, and during specialization of the same
468 pathogen to different hosts[54–56]. The evolution of worm genomes to species-specific

parasitism has also been reported[57]. It is therefore possible that this E2 of the zoonotic *T. spiralis* parasite evolved under pressure to compete with a host ortholog whose identity is highly conserved across a wide range of mammalian species. In summary, we have discovered a novel effect of *Ts*UBE2L3 on skeletal muscle tissue, namely that it suppresses ubiquitination and degradation of skeletal muscle specific proteins, thus having a stabilizing effect. Muscular degenerative diseases often involve the loss of muscle mass, structure and function as a result of the breakdown of proteins such as myosins. The Ub/proteasome system plays a key role in this pathology[58,59]. Since treatment of these disorders could involve the stabilization of these degradative pathways, we are led to speculate on the therapeutic potential of *Ts*UBE2L3. Most parasitic worm-derived therapeutics are products involved in immuno-regulation, since many of these parasites have been found to skew the mammalian immune response towards one that is beneficial in allergic and autoimmune disorders[60–62]. However there are some parasite-derived mammalian cell modulators whose (non-immuno) activity is also being investigated for medical purposes[63]. Given the chronic infections many parasites establish and their specialized tissue tropism within the host, a better understanding of their cell biology could yield insight into novel treatments for unrelated, non-infectious diseases.

Experimental procedures

For detailed experimental methods and primer sequences please refer to Supplemental Experimental Procedures

Collection and analysis of *T.spiralis* secreted proteins

T. spiralis L1-stage muscle larvae were isolated from infected rat skeletal muscle tissue (Sprague-Dawley, Harlan UK LTD, Bicester OX25 1TP) by digestion with acidified pepsin and secreted products (SP) were collected as described by Arden et al[64]. Protein concentrations were normalized by BCA assay (Pierce) and either separated by SDS-PAGE and manually extracted from the gel or precipitated by trichloroacetic acid using standard methods.

LC/MS/MS

Samples were digested with trypsin using standard protocols and peptides were analyzed on either an Orbitrap XL2 (*T. spiralis* SP) or Elite (co-IP) mass spectrometer. MS2 spectra were searched using SEQUEST v.28 against a composite database derived from the UniProt *Trichinella spiralis* proteome, its reversed complement and known contaminants. Peptide spectral matches were filtered to either a 1% (*T. spiralis* SP) false discovery rate (FDR) or a 1.7% FDR (co-IP) using the target-decoy strategy combined with linear discriminant analysis.

***Ts*UBE2L3 depletion and Ub conjugation assays**

T. spiralis SP were depleted of *Ts*UBE2L3 by incubating with Dynabead-bound (Life Technologies)-anti-*Hs*UBE2L3 antibodies. Bound proteins were eluted with glycine elution and refolded into Ub assay buffer. For parkin auto-ubiquitination assays, reactions were initiated using the Boston Biochem K105 kit according to the manufacturer's instructions and p-parkin (kindly donated by Wade Harper and Alban Ordureau, Harvard Medical School)[65]. Reaction mixtures were initiated by addition of biotin-Ub:Ub and incubated at 37°C for 1.5 h. Proteins were separated by SDS-PAGE and analyzed by streptavidin-blot.

521

522 **Generation and differentiation of C2C12 cell lines**

523 PLVX Tet On (1 ml) and pLVX Tight Puro lentivirus particles were prepared in HEK 293T
524 cells (ATCC) as described by Mostoslavsky et al[66]. Stable transgenic C2C12 (ATCC)
525 cell lines were generated by spinfection using equal volumes of Tet On and Tight Puro
526 particles added with 8 µg/ml Polybrene (Sigma) to cells at 70% confluency. Stable
527 C2C12 cell lines were drug selected and differentiated into myotubes before transgene
528 induction using 2 µg/ml doxycycline (DOX).

529

530 **Preparation of myotube lysates and co-immuno-precipitation**

531 Nuclear and cytosolic extracts were prepared using the CelLyic NuCLEAR Extraction kit
532 (Sigma-Aldrich) according to the manufacturer's instructions. The cytosolic and nuclear
533 fractions of each sample were pooled and protein concentrations normalized by BCA
534 assay. Proteins were immunoprecipitated using anti-HA affinity matrix (Roche) and HA
535 peptide elution. Supernatants were pooled for SDS-PAGE, silver staining and
536 LC/MS/MS analysis.

537

538 **Yeast-2-hybrid (Y2H) analysis**

539 Human E3-RING prey clones were constructed as described previously[32,33] using
540 pACTBD/E-B vectors[67]. The *Ts*UBE2L3 open reading frame was cloned from
541 pGEMTeasy into the bait pGBAE-B Y2H vector through *in vivo* gap repair cloning as
542 previously described[67,68]. The *Ts*UBE2L3 bait clone was mated against arrays of 166
543 full-length CDS human E3-RING prey clones and 39 prey clones containing the
544 cytoplasmic domains of human transmembrane E3-RING proteins. Growth of positive
545 colonies was monitored and scored over a period of 14 days (Figure S6 and Table S1).

546

UbiScan: LC/MS/MS

UbiScan analysis was carried out by Cell Signaling Technology as previously described[69–71] and LC/MS/MS was carried out on enriched trypsin-digested Ub peptides. MS/MS spectra were evaluated using SEQUEST and the Core platform from Harvard University[37,38,72]. Searches were performed against the most recent update of the NCBI *Mus musculus* database with mass accuracy of +/-5 ppm for precursor ions and 1 Da for product ions. Results were filtered for the presence of the intended motif (K-εGG).

Acknowledgments:

We thank the following for their kind contributions: Kleoniki Gounaris for *Trichinella* expertise, Wade Harper and Alban Ordureau for parkin protein, Andrew Blagborough for eGFP plasmids and Lorraine Lawrence for assistance with IHF.

References:

1. Hershko A, Ciechanover A. The ubiquitin system. Annu Rev Biochem. 1998;67:425–79.

2. Kerscher O, Felberbaum R, Hochstrasser M. Modification of proteins by ubiquitin and ubiquitin-like proteins. Annu Rev Cell Dev Biol. 2006;22:159–80.

3. Ardley HC, Robinson PA. E3 ubiquitin ligases. Essays Biochem. 2005;41:15–30.

4. Ciechanover A. The ubiquitin–proteasome pathway: on protein death and cell life.

EMBO J. EMBO Press; 1998 Dec 15;17(24):7151–60.

5. Hochstrasser M. Ubiquitin signalling: what's in a chain? Nat Cell Biol. 2004 Jul;6(7):571–2.

6. Ye Z, Petrof EO, Boone D, Claud EC, Sun J. Salmonella effector AvrA regulation of colonic epithelial cell inflammation by deubiquitination. Am J Pathol. 2007 Sep;171(3):882–92.

7. Zhang Y, Higashide WM, McCormick BA, Chen J, Zhou D. The inflammation-associated Salmonella SopA is a HECT-like E3 ubiquitin ligase. Mol Microbiol. 2006 Nov;62(3):786–93.

8. Loureiro J, Ploegh HL. Antigen Presentation and the Ubiquitin-Proteasome System in Host–Pathogen Interactions. In: Advances in Immunology. Academic Press; 2006. p. 225–305.

9. Angot A, Vergunst A, Genin S, Peeters N. Exploitation of eukaryotic ubiquitin signaling pathways by effectors translocated by bacterial type III and type IV secretion systems. PLoS Pathog. 2007 Jan;3(1):e3.

10. Bougdour A, Durandau E, Brenier-Pinchart M-P, Ortet P, Barakat M, Kieffer S, et al. Host cell subversion by Toxoplasma GRA16, an exported dense granule protein that targets the host cell nucleus and alters gene expression. Cell Host Microbe. 2013 Apr 17;13(4):489–500.

11. Hashimoto M, Murata E, Aoki T. Secretory protein with RING finger domain (SPRING) specific to Trypanosoma cruzi is directed, as a ubiquitin ligase related protein, to the nucleus of host cells. Cell Microbiol. 2010 Jan;12(1):19–30.

12. Wu Z, Nagano I, Boonmars T, Takahashi Y. A spectrum of functional genes mobilized after Trichinella spiralis infection in skeletal muscle. Parasitology. 2005 May;130(Pt 5):561–73.

13. Dabrowska M, Skoneczny M, Zielinski Z, Rode W. Nurse cell of Trichinella spp. as a model of long-term cell cycle arrest. Cell Cycle. 2008 Jul 15;7(14):2167–78.

14. Bai X, Wu X, Wang X, Liu X, Song Y, Gao F, et al. Inhibition of mammalian muscle differentiation by excretory secretory products of muscle larvae of Trichinella spiralis in vitro. Parasitol Res. 2012 Jun;110(6):2481–90.

15. Despommier D. Adaptive changes in muscle fibers infected with Trichinella spiralis. Am J Pathol. 1975 Mar;78(3):477–96.

16. Jasmer DP. Trichinella spiralis: altered expression of muscle proteins in trichinosis. Exp Parasitol. 1990 May;70(4):452–65.

17. Robinson MW, Greig R, Beattie KA, Lamont DJ, Connolly B. Comparative analysis of the excretory-secretory proteome of the muscle larva of Trichinella pseudospiralis and Trichinella spiralis. Int J Parasitol. 2007 Feb;37(2):139–48.

18. Robinson MW, Connolly B. Proteomic analysis of the excretory-secretory proteins of the Trichinella spiralis L1 larva, a nematode parasite of skeletal muscle. Proteomics. Wiley Online Library; 2005;5(17):4525–32.

19. Robinson MW, Gare DC, Connolly B. Profiling excretory/secretory proteins of Trichinella spiralis muscle larvae by two-dimensional gel electrophoresis and mass spectrometry. Vet Parasitol. 2005 Sep 5;132(1-2):37–41.

20. Robinson MW, Massie DH, Connolly B. Secretion and processing of a novel multi-

615 domain cystatin-like protein by intracellular stages of Trichinella spiralis. Mol
616 Biochem Parasitol. 2007 Jan;151(1):9–17.

617 21. Selkirk ME, Hussein AS, Chambers AE, Goulding D, Gares M-P, Vásquez-Lopez C,
618 et al. Trichinella spiralis secretes a homologue of prosaposin. Mol Biochem
619 Parasitol. 2004 May;135(1):49–56.

620 22. Romaris F, North SJ, Gagliardo LF, Butcher BA, Ghosh K, Beiting DP, et al. A
621 putative serine protease among the excretory–secretory glycoproteins of L1
622 Trichinella spiralis. Mol Biochem Parasitol. 2002 Jul;122(2):149–60.

623 23. Bruce AF, Gounaris K. Characterisation of a secreted N-acetyl-beta-
624 hexosaminidase from Trichinella spiralis. Mol Biochem Parasitol. 2006
625 Jan;145(1):84–93.

626 24. Gounaris K, Selkirk ME, Sadeghi SJ. A nucleotidase with unique catalytic properties
627 is secreted by Trichinella spiralis. Mol Biochem Parasitol. 2004 Aug;136(2):257–64.

628 25. Guiliano DB, Oksov Y, Lustigman S, Gounaris K, Selkirk ME. Characterisation of
629 novel protein families secreted by muscle stage larvae of Trichinella spiralis. Int J
630 Parasitol. 2009 Apr;39(5):515–24.

631 26. Horton P, Park K-J, Obayashi T, Fujita N, Harada H, Adams-Collier CJ, et al. WoLF
632 PSORT: protein localization predictor. Nucleic Acids Res. 2007 Jul;35(Web Server
633 issue):W585–7.

634 27. Nakai K, Horton P. PSORT: a program for detecting sorting signals in proteins and
635 predicting their subcellular localization. Trends Biochem Sci. 1999 Jan;24(1):34–6.

636 28. Petersen TN, Brunak S, von Heijne G, Nielsen H. SignalP 4.0: discriminating signal

peptides from transmembrane regions. Nat Methods. 2011 Sep 29;8(10):785–6.

29. Blumenfeld N, Gonen H, Mayer A, Smith CE. Purification and characterization of a novel species of ubiquitin-carrier protein, E2, that is involved in degradation of non-“ N-end rule” protein substrates. Journal of Biological [Internet]. ASBMB; 1994; Available from: http://www.jbc.org/content/269/13/9574.short

30. Blau HM, Pavlath GK, Hardeman EC, Chiu CP, Silberstein L, Webster SG, et al. Plasticity of the differentiated state. Science. 1985 Nov 15;230(4727):758–66.

31. Yaffe D, Saxel O. Serial passaging and differentiation of myogenic cells isolated from dystrophic mouse muscle. Nature. 1977;270(5639):725–7.

32. Markson G, Kiel C, Hyde R, Brown S, Charalabous P, Bremm A, et al. Analysis of the human E2 ubiquitin conjugating enzyme protein interaction network. Genome Res. 2009 Oct;19(10):1905–11.

33. Woodsmith J, Jenn RC, Sanderson CM. Systematic analysis of dimeric E3-RING interactions reveals increased combinatorial complexity in human ubiquitination networks. Mol Cell Proteomics. 2012 Jul;11(7):M111.016162.

34. Ardley HC, Tan NG, Rose SA, Markham AF, Robinson PA. Features of the parkin/ariadne-like ubiquitin ligase, HHARI, that regulate its interaction with the ubiquitin-conjugating enzyme, Ubch7. J Biol Chem. 2001 Jun 1;276(22):19640–7.

35. Krissinel E, Henrick K. Inference of macromolecular assemblies from crystalline state. J Mol Biol. 2007 Sep 21;372(3):774–97.

36. Pires DEV, Ascher DB, Blundell TL. mCSM: predicting the effects of mutations in proteins using graph-based signatures. Bioinformatics. 2014 Feb 1;30(3):335–42.

37. Huttlin EL, Jedrychowski MP, Elias JE, Goswami T, Rad R, Beausoleil SA, et al. A tissue-specific atlas of mouse protein phosphorylation and expression. Cell. 2010 Dec 23;143(7):1174–89.

38. Villén J, Beausoleil SA, Gerber SA, Gygi SP. Large-scale phosphorylation analysis of mouse liver. Proceedings of the National Academy of Sciences. 2007 Jan 30;104(5):1488–93.

39. Frickel E-M, Quesada V, Muething L, Gubbels M-J, Spooner E, Ploegh H, et al. Apicomplexan UCHL3 retains dual specificity for ubiquitin and Nedd8 throughout evolution. Cell Microbiol. 2007 Jun;9(6):1601–10.

40. Morrow ME, Kim M-I, Ronau JA, Sheedlo MJ, White RR, Chaney J, et al. Stabilization of an unusual salt bridge in ubiquitin by the extra C-terminal domain of the proteasome-associated deubiquitinase UCH37 as a mechanism of its exo specificity. Biochemistry. 2013 May 21;52(20):3564–78.

41. Pereira RV, de S Gomes M, Olmo RP, Souza DM, Cabral FJ, Jannotti-Passos LK, et al. Ubiquitin-specific proteases are differentially expressed throughout the Schistosoma mansoni life cycle. Parasit Vectors. 2015 Jun 26;8:349.

42. White RR, Miyata S, Papa E, Spooner E, Gounaris K, Selkirk ME, et al. Characterisation of the Trichinella spiralis deubiquitinating enzyme, TsUCH37, an evolutionarily conserved proteasome interaction partner. PLoS Negl Trop Dis. 2011 Oct;5(10):e1340.

43. Lin AE, Ebert G, Ow Y, Preston SP, Toe JG, Cooney JP, et al. ARIH2 is essential for embryogenesis, and its hematopoietic deficiency causes lethal activation of the immune system. Nat Immunol. 2013 Jan;14(1):27–33.

682 44. Wenzel DM, Klevit RE. Following Ariadne's thread: a new perspective on RBR
683 ubiquitin ligases. BMC Biol. 2012 Mar 15;10:24.

684 45. Marteijn JA, van der Meer LT, Smit JJ, Noordermeer SM, Wissink W, Jansen P, et
685 al. The ubiquitin ligase Triad1 inhibits myelopoiesis through UbcH7 and Ubc13
686 interacting domains. Leukemia. 2009 Aug;23(8):1480–9.

687 46. Abu Hatoum O, Gross-Mesilaty S, Breitschopf K, Hoffman A, Gonen H,
688 Ciechanover A, et al. Degradation of myogenic transcription factor MyoD by the
689 ubiquitin pathway in vivo and in vitro: regulation by specific DNA binding. Mol Cell
690 Biol. 1998 Oct;18(10):5670–7.

691 47. Gardrat F, Montel V, Raymond J, Azanza JL. Proteasome and myogenesis. Mol Biol
692 Rep. 1997 Mar;24(1-2):77–81.

693 48. Polge C, Attaix D, Taillandier D. Role of E2-Ub-conjugating enzymes during skeletal
694 muscle atrophy. Front Physiol. 2015 Mar 10;6:59.

695 49. Despommier DD. How does Trichinella spiralis make itself at home? Parasitol
696 Today. 1998 Aug;14(8):318–23.

697 50. Jasmer DP, Bohnet S, Prieur DJ. Trichinella spp.: differential expression of acid
698 phosphatase and myofibrillar proteins in infected muscle cells. Exp Parasitol. 1991
699 Apr;72(3):321–31.

700 51. Cohen S, Brault JJ, Gygi SP, Glass DJ, Valenzuela DM, Gartner C, et al. During
701 muscle atrophy, thick, but not thin, filament components are degraded by MuRF1-
702 dependent ubiquitylation. J Cell Biol. 2009 Jun 15;185(6):1083–95.

703 52. Polge C, Heng A-E, Jarzaguet M, Ventadour S, Claustre A, Combaret L, et al.

Muscle actin is polyubiquitinylated in vitro and in vivo and targeted for breakdown by the E3 ligase MuRF1. FASEB J. 2011 Nov;25(11):3790–802.

53. Koyama S, Hata S, Witt CC, Ono Y, Lerche S, Ojima K, et al. Muscle RING-Finger Protein-1 (MuRF1) as a Connector of Muscle Energy Metabolism and Protein Synthesis. J Mol Biol. 2008 Mar 7;376(5):1224–36.

54. Rokas A, Hittinger CT. Transcriptional rewiring: the proof is in the eating. Curr Biol. 2007 Aug 21;17(16):R626–8.

55. Niu C, Yu D, Wang Y, Ren H, Jin Y, Zhou W, et al. Common and pathogen-specific virulence factors are different in function and structure. Virulence. 2013 Aug 15;4(6):473–82.

56. El-Sayed NM, Myler PJ, Blandin G, Berriman M, Crabtree J, Aggarwal G, et al. Comparative genomics of trypanosomatid parasitic protozoa. Science. 2005 Jul 15;309(5733):404–9.

57. Tsai IJ, Zarowiecki M, Holroyd N, Garciarrubio A, Sanchez-Flores A, Brooks KL, et al. The genomes of four tapeworm species reveal adaptations to parasitism. Nature. 2013 Apr 4;496(7443):57–63.

58. Peterson JM, Bakkar N, Guttridge DC. NF-κB signaling in skeletal muscle health and disease. Curr Top Dev Biol. 2011;96:85–119.

59. Shintaku J, Guttridge DC. Reining in nuclear factor-kappaB in skeletal muscle disorders. Curr Opin Clin Nutr Metab Care. 2013 May;16(3):251–7.

60. Elliott DE, Weinstock JV. Helminthic Therapy: Using Worms to Treat Immune-Mediated Disease. In: Pathogen-Derived Immunomodulatory Molecules. Springer

New York; 2009. p. 157–66. (Advances in Experimental Medicine and Biology).

61. Harnett W, Harnett MM. Helminth-derived immunomodulators: can understanding the worm produce the pill? Nat Rev Immunol. 2010 Apr;10(4):278–84.

62. van Riet E, Hartgers FC, Yazdanbakhsh M. Chronic helminth infections induce immunomodulation: consequences and mechanisms. Immunobiology. 2007 Apr 20;212(6):475–90.

63. Pérez-Torres A, Vera-Aguilera J, Hernaiz-Leonardo JC, Moreno-Aguilera E, Monteverde-Suarez D, Vera-Aguilera C, et al. The synthetic parasite-derived peptide GK1 increases survival in a preclinical mouse melanoma model. Cancer Biother Radiopharm. 2013 Nov;28(9):682–90.

64. Arden SR, Smith AM, Booth MJ, Tweedie S, Gounaris K, Selkirk ME. Identification of serine/threonine protein kinases secreted by Trichinella spiralis infective larvae. Mol Biochem Parasitol. 1997 Dec 1;90(1):111–9.

65. Ordureau A, Sarraf SA, Duda DM, Heo J-M, Jedrychowski MP, Sviderskiy VO, et al. Quantitative proteomics reveal a feedforward mechanism for mitochondrial PARKIN translocation and ubiquitin chain synthesis. Mol Cell. 2014 Nov 6;56(3):360–75.

66. Mostoslavsky G, Kotton DN, Fabian AJ, Gray JT, Lee J-S, Mulligan RC. Efficiency of transduction of highly purified murine hematopoietic stem cells by lentiviral and oncoretroviral vectors under conditions of minimal in vitro manipulation. Mol Ther. 2005 Jun;11(6):932–40.

67. Semple JI, Prime G, Wallis LJ, Sanderson CM, Markie D. Two-hybrid reporter vectors for gap repair cloning. Biotechniques. 2005 Jun;38(6):927–34.

68. Ito H, Fukuda Y, Murata K, Kimura A. Transformation of intact yeast cells treated with alkali cations. J Bacteriol. 1983 Jan;153(1):163–8.

69. Guo A, Gu H, Zhou J, Mulhern D, Wang Y, Lee KA, et al. Immunoaffinity enrichment and mass spectrometry analysis of protein methylation. Mol Cell Proteomics. 2014 Jan;13(1):372–87.

70. Lee KA, Hammerle LP, Andrews PS, Stokes MP, Mustelin T, Silva JC, et al. Ubiquitin ligase substrate identification through quantitative proteomics at both the protein and peptide levels. J Biol Chem. 2011 Dec 2;286(48):41530–8.

71. Rush J, Moritz A, Lee KA, Guo A, Goss VL, Spek EJ, et al. Immunoaffinity profiling of tyrosine phosphorylation in cancer cells. Nat Biotechnol. 2005 Jan;23(1):94–101.

72. Eng JK, McCormack AL, Yates JR. An approach to correlate tandem mass spectral data of peptides with amino acid sequences in a protein database. J Am Soc Mass Spectrom. 1994 Nov;5(11):976–89.

764 **Figure and Table legends:**

765

766 **Figure 1.** *Identification of E2 and E3 activity in T. spiralis SP.* **A.** Streptavidin-HRP blot of
767 *in vitro* ubiquitination reactions including 1) human E1 (UBE1A), E2 (UBE2L3), E3
768 (parkin), and Ub-biotin, 2) in the absence of the E2, 3) SP substituted for the human E2,
769 4) SP substituted for the human E3, 5) SP substituted for the human E1, 6) SP
770 substituted for both the human E2 and E3, 7) SP and Ub-biotin alone. **B.** *T.sp* SP were
771 separated by SDS-PAGE and visualized by silver-staining. 50 µg of SP were de-
772 glycosylated by PNGase treatment and analyzed by LC/MS/MS (10 µg of glycosylated
773 proteins were analyzed for comparison). Peptides matching a *T. spiralis* E2, *Ts*UBE2L3,
774 were identified from the boxed section of the gel.

775

776 **Figure 2.** *Verification of expression, secretion, activity and localization of TsUBE2L3.* **A**.
777 *T.sp* SP, HEK 293T cell lysate and *T. spiralis* muscle larvae lysate were separated by
778 SDS-PAGE and immuno-blotted with anti-*Hs*UBE2L3 and anti-tubulin antibodies . **B.**
779 Auto-ubiquitination of parkin with Ub-biotin was probed by streptavidin-HRP blot.
780 Reactions from left to right: lane 1: human E1 (UBE1A), E3 (parkin) and Ub-biotin only
781 (no E2). Reactions in lanes 2-4 included human E1, parkin and Ub-biotin, with the
782 following E2 substitution: lane 2: *T.sp* SP after resin-bound BSA depletion (BSA), lane 3:
783 *T.sp* SP after resin-bound anti-tubulin depletion (α-tubulin), lane 4: *T.sp* SP after resin-
784 bound α-*Hs*UBE2L3 depletion (α-*Hs*UBE2L3). In lanes 5-7 the elution fractions from the
785 depletions shown in lanes 2-4 were used to substitute E2. **C**. The pixel intensity of lanes
786 2-7 of the depletion assay (B) was analysed using an ImageJ gel analysis plugin. For
787 each of the three samples tested in the assay (BSA, α-tubulin and α-*Hs*UBE2L3) the
788 sum of the pixel intensity of the depletion plus elution lanes was taken as 100%
789 (intensity of lane 2 + 5 for BSA and so on). The relative percentages of the depletion and

elution lanes were then calculated (intensity of lane 2/(2+5) x 100) and plotted. **D**. A *Ts*UBE2L3-specific antibody was made and its specificity was assessed by immuno-blot against *T.sp* L1 lysate, *T.sp* SP and rat (*R.n*) skeletal muscle tissue (SMT) lysate. The arrow indicates the expected size of *Ts*UBE2L3. **E.** *T. spiralis* infected rat skeletal muscle tissue (R.n SMT) was sectioned and analyzed by immuno-histofluorescence . A single *T.sp* L1 inside the nurse cell (n), surrounded by a collagen capsule (c) is displayed. Tissue was probed with anti-*Ts*UBE2L3 antibodies (Alexa-568, red) and nuclei were stained using DAPI (blue). Brightfield (BF)/DAPI/anti-*Ts*UBE2L3 and DAPI/anti-*Ts*UBE2L3 merged images are displayed. As a control, infected *R.n*SMT was probed with PBS and DAPI only. Arrows indicate stacks of stichocyte cells in the stichosome. **F.** Annotated diagram of *T. spiralis* L1 morphology. Image adapted from a drawing by Villella, J.B. (1970, Life cycle and morphology, in: Trichinosis in Man and Animals (S.E. Gould, ed.), Charles C. Thomas, Springfield, Illinois, pp. 19-60,) taken from *Trichinella*.org/biology.

Figure 3. *Development of expression system for TsUBE2L3 analysis in C2C12 myotubes.* **A**. Wild-type C2C12 undifferentiated myoblasts and terminally differentiated myotubes were probed by immuno-fluorescence (IFA) with anti-tubulin antibodies (Alexa-488, green) and nuclei were stained with DAPI (blue). **B.** Schematic of the pLVX expression construct containing the coding sequence for *Ts*UBE2L3-HA, showing the mechanism of induction by doxycycline (DOX). **C**. Myotubes transduced with empty vector pLVX or *Ts*UBE2L3-HA pLVX and induced with DOX for 24 h were probed by IFA with anti-HA antibodies (Alexa-568, red); nuclei were stained with DAPI (blue). **D**. Empty vector and *Ts*UBE2L3-HA cell lysates were reacted with myogenic differentiation markers, myogenin and myosin heavy chain II (MHC), and anti-HA antibodies, at indicated time points after 24 h DOX induction and analyzed by immuno-blot. The same

816 samples were probed with anti-tubulin as a loading control.

817

818 **Figure 4.** *Co-immuno-precipitation (co-IP) and yeast-2-hybrid (Y2H) analyses of*
819 *TsUBE2L3.* **A.** Transgenic C2C12 myotube lines (empty vector, eGFP-HA, *Ts*UBE2L3-
820 HA and mouse *Mm*UBE2L3-HA) after 24 h DOX induction were probed by co-IP with
821 anti-HA antibody. Co-IP elutions were silver-stained and all co-IP'd proteins were
822 analyzed by LC/MS/MS. The same samples were reacted with anti-HA antibodies by
823 immuno-blot (IB) as a control for transgene expression. **B**. Protein interaction network
824 showing positive interactions between *Ts*UBE2L3 and human E3 ligases as observed by
825 yeast-2-hybrid (Y2H) and co-IP analyses. Key indicates if interactions were found by
826 Y2H to be strong, weak or by co-IP.

827

828 **Table 1.** *Identification of TsUBE2L3 E3 interaction partners by co-IP and yeast-2-hybrid*
829 *(Y2H) analyses.* Only interactions measured by Y2H as being strong are listed. Known
830 ubiquitination substrates found by UbiScan analysis to be significantly and specifically
831 upregulated (upreg.) or downregulated (downreg.) after expression of *Ts*UBE2L3-HA are
832 listed.

833

834 **Figure 5.** *Expression, purification and activity of 6His-TsUBE2L3 and 6His-ARIH2 in*
835 *vitro.* **A**. Coommassie stain of 6His-*Ts*UBE2L3 from un-induced (UI) and induced (I)
836 *E.coli* cultures, nickel purification resin flow-through (FT1-2), wash (W) and elutions (E1-
837 2). **B and D**. Streptavidin-HRP blots of *in vitro* parkin auto-ubiquitination reactions using
838 human E1 (UBE1A), human Ub-biotin and either no E2, human E2 (*Hs*UBE2L3) or 6His-
839 *Ts*UBE2L3 with **(B)** human parkin as the E3 or **(C)** human ARIH2 as the E3. **C.**
840 Coomassie stain of 6His-*Hs*ARIH2ΔAri from un-induced (UI) *E.coli* cultures, inclusion
841 body supernatants (S1-4) induced inclusion bodies (I) and refolded from inclusion bodies

(Rf). **E.** Surface representation of ARIH2 (grey) and Ub (wheat) with *Hs*ARIH2 (green) and *Ts*UBE2L3 (cyan) bound to the RING1 domain of ARIH2. Residue differences between the E2-E3 interfaces are shown as sticks (*Hs*ARIH2 in orange and *Ts*UBE2L3 in magenta). Zinc ions are shown as blue spheres, and Val141 of ARIH2 is shown as sticks. **F**. Zoom of the ARIH2:E2:Ub interface.

Figure 6. *UbiScan analysis of TsUBE2L3 effect on the myotube ubiquitome*. **A**. Heatmap displaying proteins in which ubiquitinated peptides were found to be upregulated (blue) or downregulated (red) as measured by a fold change in relation to the empty vector C2C12 myotube cell line after 24 h expression of eGFP-HA (GFP), *Ts*UBE2L3-HA (TsE2) or *Mm*UBE2L3-HA (MmE2). Proteins listed showed a maximum % CV of 49.9 or less, a maximum intensity of 200,000 or more and a fold change in ubiquitination of 2.5 or more in response to *Ts*UBE2L3-HA expression only. Where multiple ubiquitinated peptides were identified for the same protein (according to the protein description as assigned by Cell Signaling Technology), the mean fold change was calculated. Proteins were grouped according to annotated biological ontology. **B**. Myosin II/fast skeletal myosin (MYH2) (the protein with the largest significant fold change specifically in response to *Ts*UBE2L3 expression) was analyzed by immuno-blot in the empty vector and *Ts*UBE2L3 C2C12 myotube cell lines before and after 24 h of induction (DOX) using anti-myosin II antibodies and anti-vinculin as a loading control.

Figure S1, related to Figure 1 and 2. Race confirmation of *Ts*UBE2L3 3' ORF. The RACE-PCR sequencing data of the 3' end of *Ts*UBE2L3 cDNA aligned with the annotated fragment coding sequence that is currently found in the NCBI database. Figure shows the position of the RACE oligo, the RACE 3' forward primer-binding site, the stop site of the full coding sequence of the gene, the custom gene-specific forward

primer (GSFP)-binding site and the cloning vector (pGEMTeasy) sequences. The sequence contained a 3' continuation after the stop codon that was identified as *T. spiralis* genomic DNA (gDNA).

Figure S2, related to Figure 1 and 2. Race confirmation of *Ts*UBE2L3 5' ORF. The RACE-PCR sequencing data of the 5' end of *Ts*UBE2L3 cDNA aligned with the annotated fragment coding sequence that is currently found in the NCBI database. Figure shows the position of the RACE oligo, the RACE 5' forward primer-binding site, the start site of the full coding sequence of the gene, the custom gene-specific reverse primer (GSRP)-binding site and the cloning vector (pGEMTeasy) sequence.

Figure S3, related to Figure 1 and 2. *Ts*UBE2L3 alignments. The annotated fragment (incomplete) coding sequence (cds) for *Ts*UBE2L3 (GI:339240046/*Ts*p_00154/UniProt: E5S8T6 - found in the contig sequence: GI:316975344) that is currently found in the NCBI database was aligned with the full RACE-PCR confirmed sequence from start to stop, compiled from both 5' RACE-PCR and 3' RACE-PCR data, and with the human UBE2L3 isoforms #1, #3 and #4 cds' (GI:4507789, GI:373432682 and GI:373432684 respectively-Uniprot: P68036).

Figure S4, related to Figure 3. IFA of transgenic TsUBE2L3-HA C2C12 cells. IFA of transgenic *Ts*UBE2L3-HA C2C12 undifferentiated myoblasts and differentiated myotubes showing Alexa-488 conjugated anti-HA (green), DAPI-stained nuclei (blue), brightfield (BF) and overlay (merge of three signals). Row 1 shows myoblasts with cytoplasmic *Ts*UBE2L3-HA localization in a myoblast. Row 2 shows cytoplasmic and nuclear *Ts*UBE2L3-HA localization in myoblasts. Row 3 shows only cytoplasmic *Ts*UBE2L3-HA localization in myotubes. Images are representative of multiple biological

894 replicates.

895

896 **Figure S5, related to Figure 3. IFA of transgenic (eGFP-HA and *Ts*UBE2L3-HA)**
897 **C2C12 cell lines.** IFA of anti-tubulin showing no overall morphological/shape change of
898 cells.

899

900 **Figure S6, related to Figure 4. Yeast-2-hybrid (Y2H) raw data.** Image of Y2H plates
901 (all included in screen-positive and negative). Targeted Y2H matrix mating assays
902 screening *Ts*UBE2L3 against arrays of full length and truncated E3-RING proteins (for
903 layout see Sup Table 1). Yeast growth indicates positive protein-protein interaction. 0-5
904 colonies: background yeast growth, 6-20 colonies: weak interaction, 20-200 colonies:
905 medium interaction, full plaque: strong interaction. Interactions observed only with the
906 Ade2 reporter (SD-WLA) are not considered true positive interactions, however those
907 with the His3 reporter only (SD-WLH(AT)) are considered positive.

908

909 **Table S1, related to Figure 4 and S4. Yeast-2-hybrid raw plate layout.** Layouts of E3-
910 RING prey arrays screened against *Ts*UBE2L3 (see Figure S2). Top and middle panel
911 contain full-length cds E3-RING prey clones, generated by Markson and Woodsmith et
912 al[32,33]. Bottom panel contains truncated transmembrane E3-RING prey clones
913 (transmembrane domains removed), generated by Jenn, R.C (unpublished data). * Non-
914 E3-RING clones in the array. Red text indicates interaction with *Ts*UBE2L3.

915

916 **Table S2, related to Figure 4. Co-IP data.** Table of co-IP data showing reference
917 results including the annotated protein sequence that is currently found in the NCBI
918 database (“ubiquitin-conjugating enzyme E2 L3, partial” GI:339240047), all E3 proteins
919 that co-IP'd with *Ts*UBE2L3-HA (as well as controls) and all proteins that only co-IP'd

with *Ts*UBE2L3-HA (and neither control). E3 ligases are highlighted in bold font.

Table S3, related to Figure 6. Raw UbiScan data. UbiScan data as generated by Cell Signaling Technology showing fold change by protein type in levels of ubiquitinated peptides in GFP, *Ts*UBE2L3 and *Mm*UBE2L3 myotubes, in relation to the empty vector control cell line.

Figure S7, related to Figure 6. A. TUBE2 IP from transgenic myotube cell lines. Anti-Ub immuno-blot showing normalized lysates of empty vector and *Ts*UBE2L3 C2C12 myotube cells (input), results of tandem ubiquitin binging entity pull-down (TUBE2), and unbound protein. An anti-vinculin immuno-blot of the same samples was included as a loading control. **B. Quantification of Ub immuno-blot.** ImageJ was used to analyze the intensity (raw pixel area) of each smear from the immuno-blot shown in A. **C. IFA of transgenic myotube cell lines.** IFA of anti-α-actinin/Alexa488 (with DAPI-stained nuclei) showing fewer ordered sarcomere A-bands in the *Ts*UBE2L3-HA cells than in the wild-type, empty vector and *Mm*UBE2L3 cells. **D**. ImageJ quantification (using the "analyze stripes" plugin) of the number of striped α-actinin-positive structures in each cell line. The mean number of stripes calculated from the analysis of 7 images (per cell line) taken over 3 independent experiments is displayed for each cell line, with error bars representing the standard error of the mean.

942 **Table 1.**

#	Mammalian E3 ligase			Identification method		E3 domain	Known Ub substrates	Human UBE2L3 interaction (literature)
	Protein name	Human protein ID (Uniprot)	Gene name(s)	Y2H strong	Co-IP			
1	ARIH1	Q9Y4X5	ARIH1, ARI, MOP6, UBCH7B, HUSSY-27, **Ariadne-1**		+	RBR	E1F4E2	+
2	**ARIH2**	**O95376**	**ARIH2, ARI2, TRIAD1, HT005, Ariadne-2**	**+**	**+**	**RBR**	**IκBβ**	**+**
3	NEDD4	P46934	NEDD4, NEDD4-1		+	HECT	IGF1R, FGFR1, TNK2, ebola virus VP40	+
4	RNF125	Q96EQ8	RNF125	+		RING	p53, p73	+
5	RNF138	Q8WVD3	RNF138, NARF, HSD-4, HSD4	+		RING	TCF/LEF	+
6	RNF14	Q9UBS8	RNF14, ARA54, HRIHFB2038	+		RBR	unknown	+
7	RNF144A	P50876	RNF144A, KIAA0161, RNF144, UBCE7IP4	+		RBR	PRKDC	+
8	RNF19A			+		RBR	SNCAIP, CASR, SOD1	+
9	RNF37	O94941	UBOX5, KIAA0860, RNF37, UBCE7IP, UIP5	+		RING	unknown	+
10	TRAF7	Q6Q0C0	TRAF7, RNF119, TNF-Rc associated-7, RFWD1		+	RING	unknown	+
11	TRIM3	O75382	TRIM3, BERP, RNF22, RNF97		+	RING	GKAP/ SAPAP1	
12	TRIM25	Q14258	TRIM25, EFP, RNF147, ZNF147		+	RING	DDX58	
13	TRIM47	Q96LD4	TRIM47, RNF100, GOA		+	RING	unknown	

943

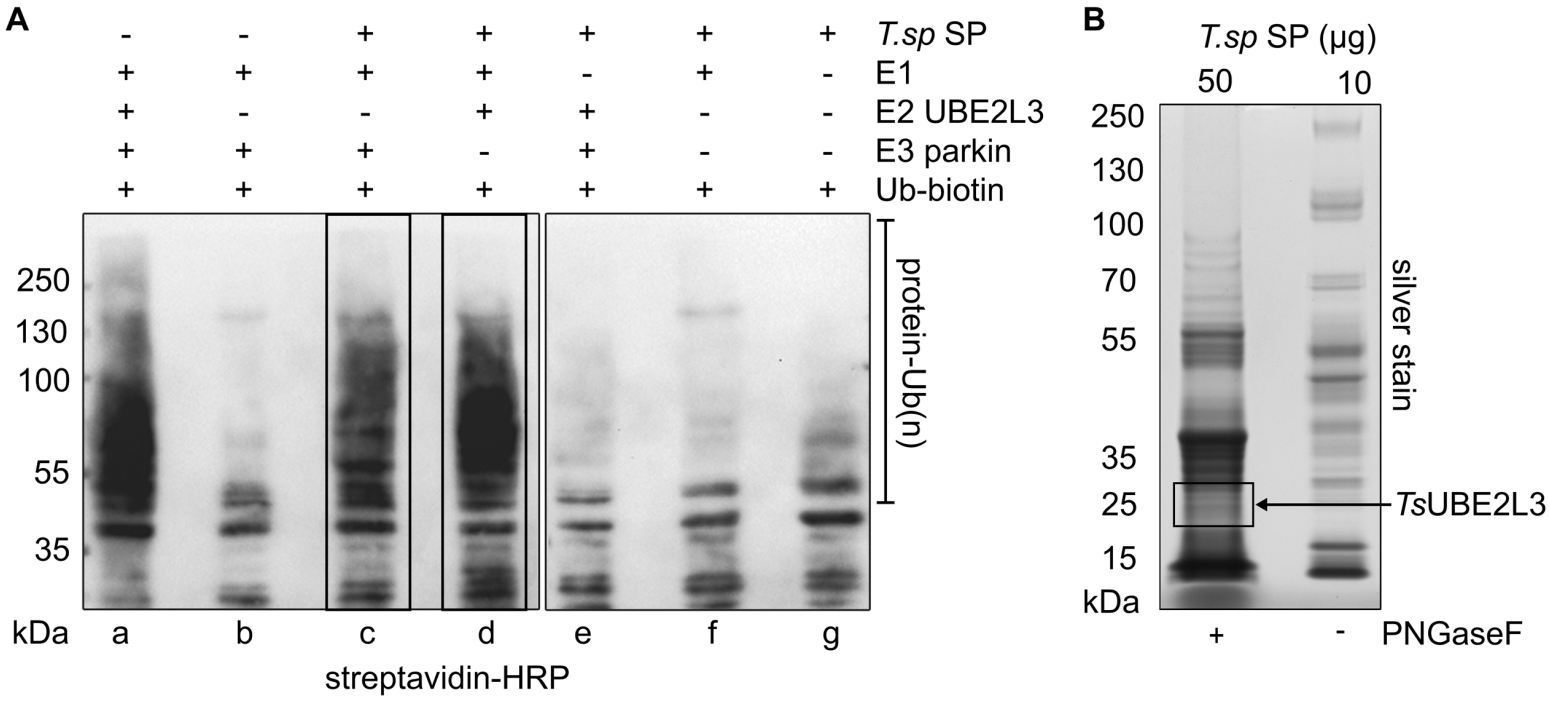
A
- - + + + + + T.sp SP
+ + + + - + - E1
+ - - + + - - E2 UBE2L3
+ + + - + - - E3 parkin
+ + + + + + + Ub-biotin
250
130
100
55
35
kDa
a
b
c
d
e
f
g
protein-Ub(n)
streptavidin-HRP
B
T.sp SP (µg)
50
10
250
130
100
70
55
35
25
15
kDa
silver stain
TsUBE2L3
+
-
PNGaseF

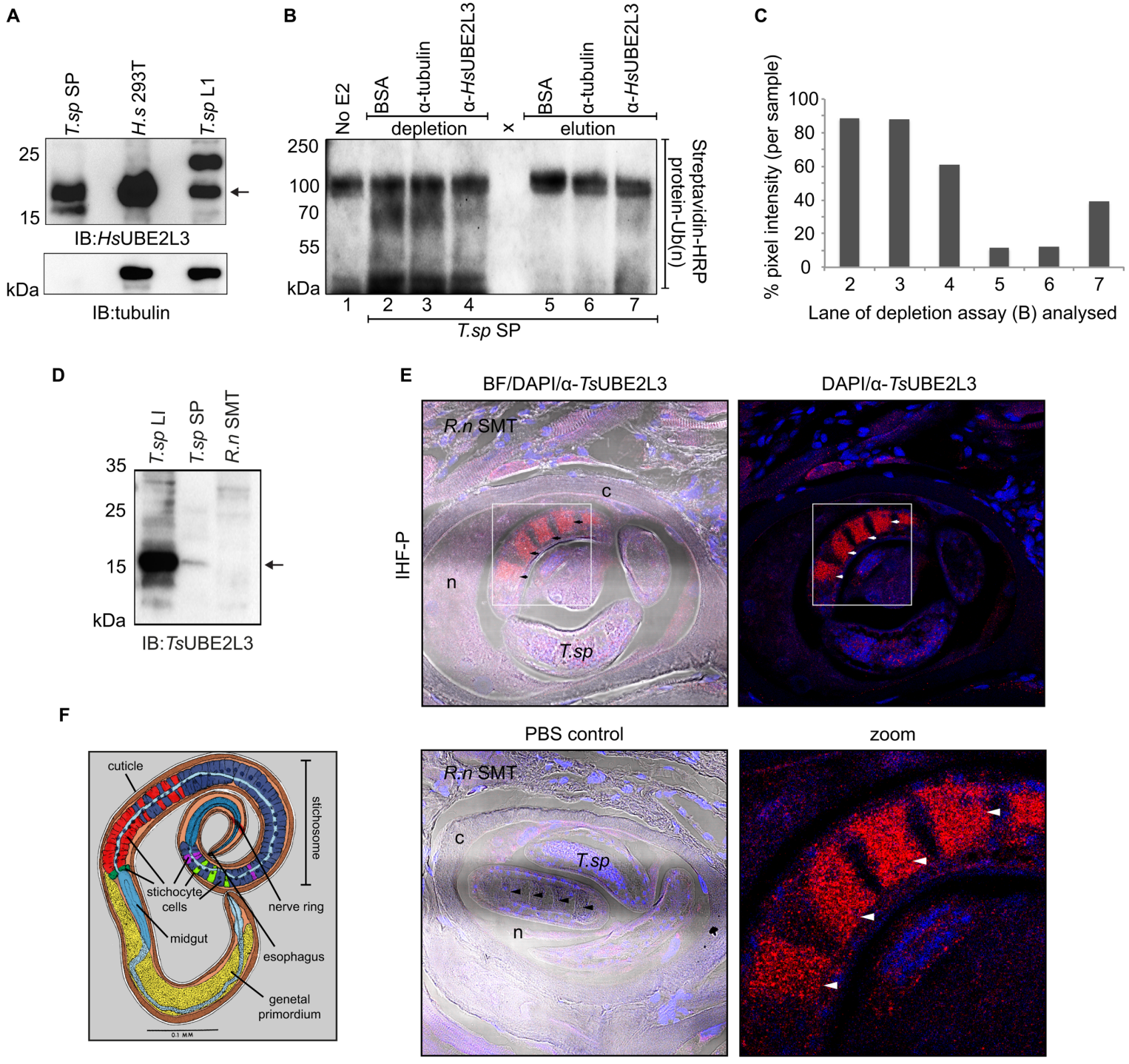
A
T.sp SP
H.s 293T
T.sp L1
25
15
IB:HsUBE2L3
kDa
IB:tubulin
B
No E2
BSA
α-tubulin
α-HsUBE2L3
depletion
x
elution
250
100
70
55
kDa
Streptavidin-HRP
protein-Ub(n)
1 2 3 4 5 6 7
T.sp SP
C
% pixel intensity (per sample)
100
80
60
40
20
0
2 3 4 5 6 7
Lane of depletion assay (B) analysed
D
T.sp LI
T.sp SP
R.n SMT
35
25
15
kDa
IB:TsUBE2L3
E
BF/DAPI/α-TsUBE2L3
DAPI/α-TsUBE2L3
IHF-P
R.n SMT
c
n
T.sp
PBS control
zoom
F
cuticle
stichosome
stichocyte cells
nerve ring
midgut
esophagus
genetal primordium
0.1 MM

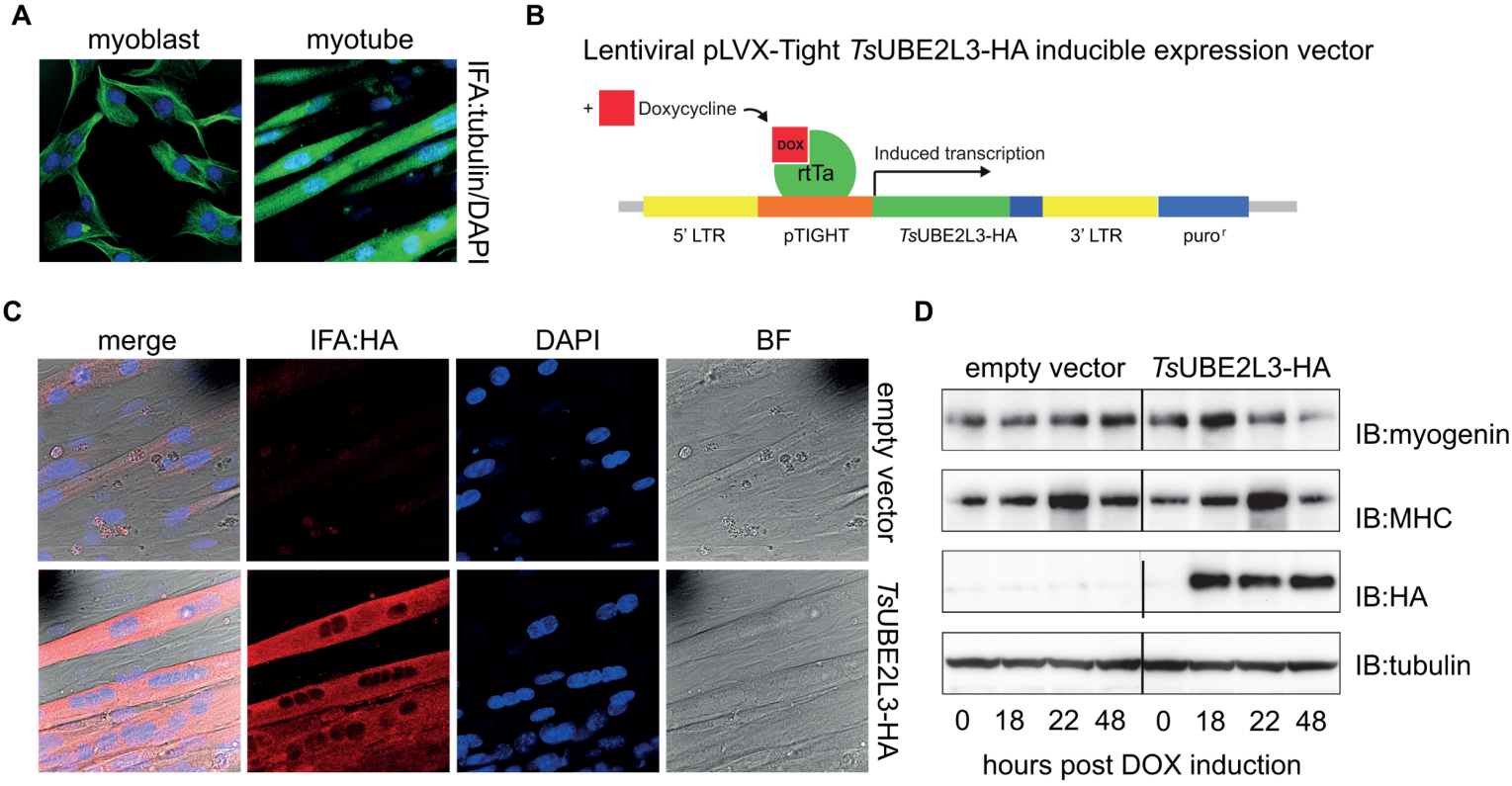
A
myoblast
myotube
IFA:tubulin/DAPI
B
Lentiviral pLVX-Tight TsUBE2L3-HA inducible expression vector
+
Doxycycline
DOX
rtTa
Induced transcription
5' LTR
pTIGHT
TsUBE2L3-HA
3' LTR
puro^r
C
merge
IFA:HA
DAPI
BF
empty vector
TsUBE2L3-HA
D
empty vector
TsUBE2L3-HA
IB:myogenin
IB:MHC
IB:HA
IB:tubulin
0 18 22 48 0 18 22 48
hours post DOX induction

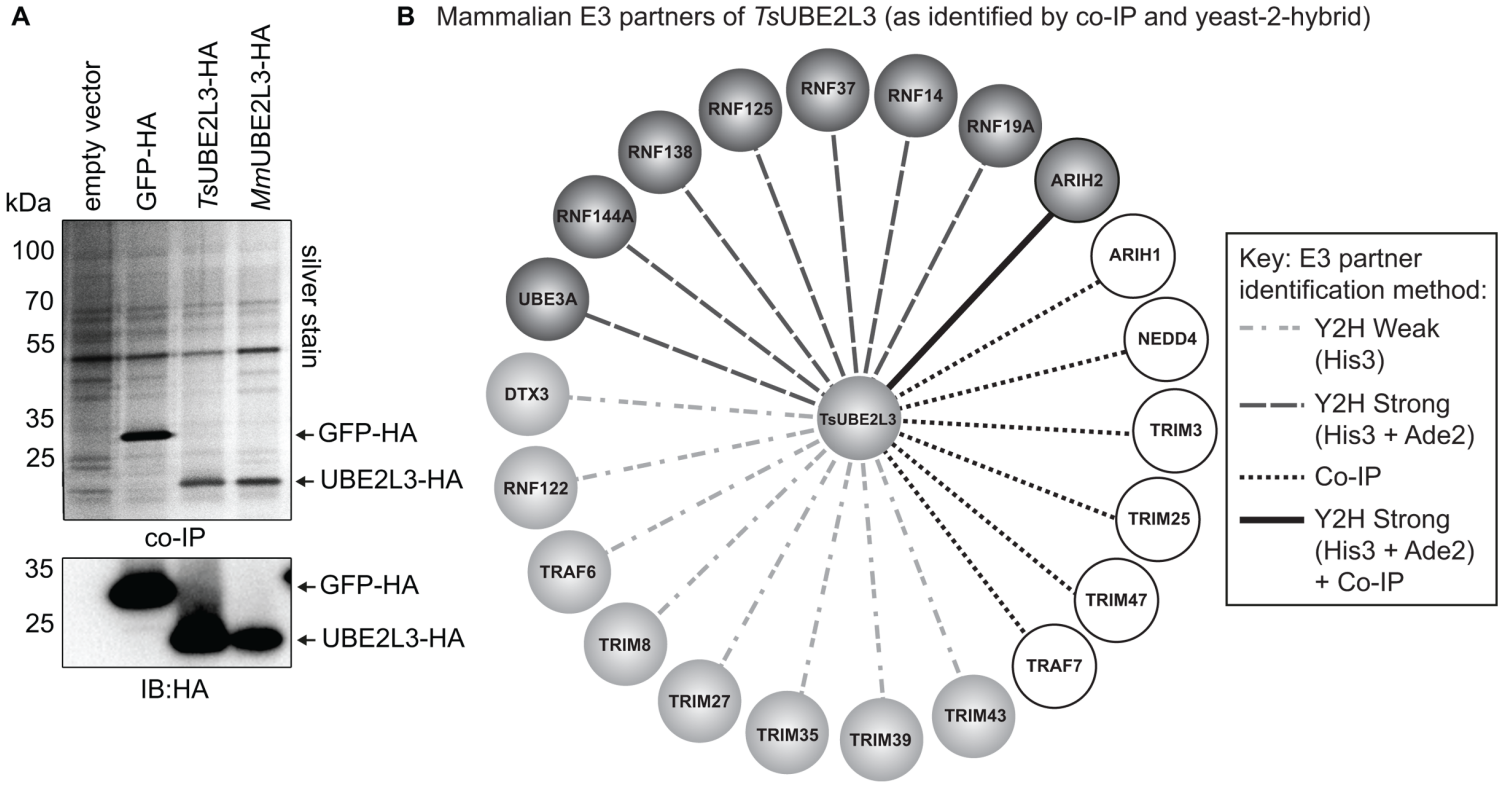
A
empty vector
GFP-HA
TsUBE2L3-HA
MmUBE2L3-HA
kDa
100
70
55
35
25
silver stain
GFP-HA
UBE2L3-HA
co-IP
35
25
GFP-HA
UBE2L3-HA
IB:HA
B
Mammalian E3 partners of TsUBE2L3 (as identified by co-IP and yeast-2-hybrid)
RNF37
RNF14
RNF125
RNF19A
RNF138
ARIH2
RNF144A
ARIH1
UBE3A
NEDD4
DTX3
TsUBE2L3
TRIM3
RNF122
TRIM25
TRAF6
TRIM47
TRIM8
TRAF7
TRIM27
TRIM35
TRIM39
TRIM43
Key: E3 partner identification method:
Y2H Weak (His3)
Y2H Strong (His3 + Ade2)
Co-IP
Y2H Strong (His3 + Ade2) + Co-IP

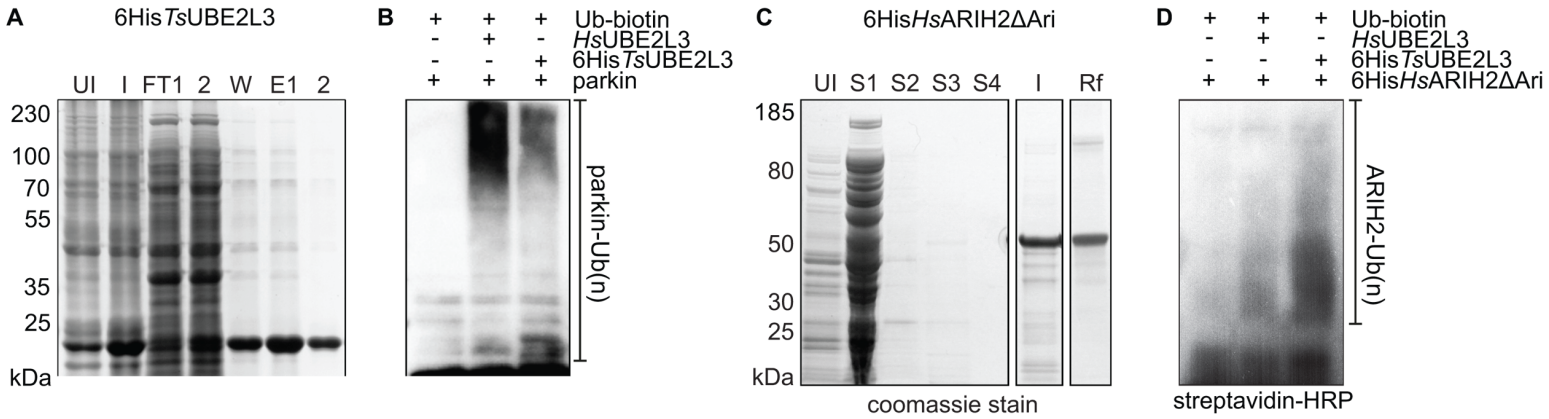
A
6His*Ts*UBE2L3
UI I FT1 2 W E1 2
230
100
70
55
35
25
kDa
B
+ + + Ub-biotin
- + - *Hs*UBE2L3
- - + 6His*Ts*UBE2L3
+ + + parkin
parkin-Ub(n)
C
6His*Hs*ARIH2ΔAri
UI S1 S2 S3 S4 I Rf
185
80
50
30
25
kDa
coomassie stain
D
+ + + Ub-biotin
- + - *Hs*UBE2L3
- - + 6His*Ts*UBE2L3
+ + + 6His*Hs*ARIH2ΔAri
ARIH2-Ub(n)
streptavidin-HRP
E
*Ts*UBE2L3
*Hs*UBE2L3
Ub
ARHI2
F
A2
T2
D13
E13
V141
Zn

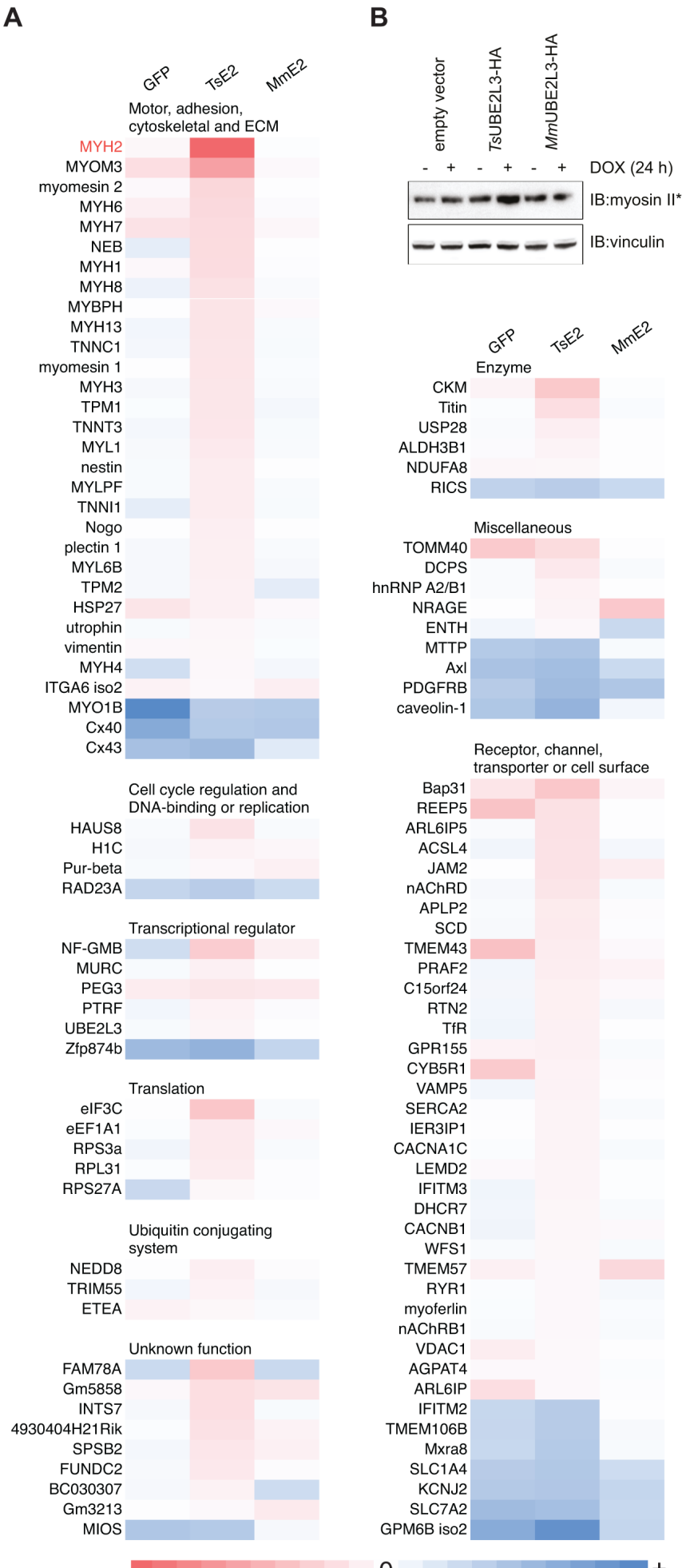
A
GFP
TsE2
MmE2
Motor, adhesion, cytoskeletal and ECM
MYH2
MYOM3
myomesin 2
MYH6
MYH7
NEB
MYH1
MYH8
MYBPH
MYH13
TNNC1
myomesin 1
MYH3
TPM1
TNNT3
MYL1
nestin
MYLPF
TNNI1
Nogo
plectin 1
MYL6B
TPM2
HSP27
utrophin
vimentin
MYH4
ITGA6 iso2
MYO1B
Cx40
Cx43
Cell cycle regulation and DNA-binding or replication
HAUS8
H1C
Pur-beta
RAD23A
Transcriptional regulator
NF-GMB
MURC
PEG3
PTRF
UBE2L3
Zfp874b
Translation
eIF3C
eEF1A1
RPS3a
RPL31
RPS27A
Ubiquitin conjugating system
NEDD8
TRIM55
ETEA
Unknown function
FAM78A
Gm5858
INTS7
4930404H21Rik
SPSB2
FUNDC2
BC030307
Gm3213
MIOS
B
empty vector
TsUBE2L3-HA
MmUBE2L3-HA
- + - + - +
DOX (24 h)
IB:myosin II*
IB:vinculin
GFP
TsE2
MmE2
Enzyme
CKM
Titin
USP28
ALDH3B1
NDUFA8
RICS
Miscellaneous
TOMM40
DCPS
hnRNP A2/B1
NRAGE
ENTH
MTTP
Axl
PDGFRB
caveolin-1
Receptor, channel, transporter or cell surface
Bap31
REEP5
ARL6IP5
ACSL4
JAM2
nAChRD
APLP2
SCD
TMEM43
PRAF2
C15orf24
RTN2
TfR
GPR155
CYB5R1
VAMP5
SERCA2
IER3IP1
CACNA1C
LEMD2
IFITM3
DHCR7
CACNB1
WFS1
TMEM57
RYR1
myoferlin
nAChRB1
VDAC1
AGPAT4
ARL6IP
IFITM2
TMEM106B
Mxra8
SLC1A4
KCNJ2
SLC7A2
GPM6B iso2
-
0
+